Cancer Cell
Article

Impaired DNA Damage Response, Genome Instability, and Tumorigenesis in SIRT1 Mutant Mice

Rui-Hong Wang,[1] Kundan Sengupta,[2] Cuiling Li,[1] Hyun-Seok Kim,[1] Liu Cao,[1] Cuiying Xiao,[1] Sangsoo Kim,[1] Xiaoling Xu,[1] Yin Zheng,[1] Beverly Chilton,[6] Rong Jia,[3] Zhi-Ming Zheng,[3] Ettore Appella,[4] Xin Wei Wang,[5] Thomas Ried,[2] and Chu-Xia Deng[1,*]
[1]Genetics of Development and Disease Branch, 10/9N105, National Institute of Diabetes and Digestive and Kidney Diseases
[2]Genetics Branch, National Cancer Institute
[3]HIV and AIDS Malignancy Branch, National Cancer Institute
[4]Laboratory of Cell Biology, National Cancer Institute
[5]Laboratory of Human Carcinogenesis, National Cancer Institute
National Institutes of Health, Bethesda, MD 20892, USA
[6]Department of Cell Biology and Biochemistry, Texas Tech University Health Science Center, Lubbock, TX 79430-6540, USA
*Correspondence: chuxiad@bdg10.niddk.nih.gov
DOI 10.1016/j.ccr.2008.09.001

SUMMARY

In lower eukaryotes, Sir2 serves as a histone deacetylase and is implicated in chromatin silencing, longevity, and genome stability. Here we mutated the *Sirt1* gene, a homolog of yeast Sir2, in mice to study its function. We show that a majority of SIRT1 null embryos die between E9.5 and E14.5, displaying altered histone modification, impaired DNA damage response, and reduced ability to repair DNA damage. We demonstrate that *Sirt1*$^{+/-}$;*p53*$^{+/-}$ mice develop tumors in multiple tissues, whereas activation of SIRT1 by resveratrol treatment reduces tumorigenesis. Finally, we show that many human cancers exhibit reduced levels of SIRT1 compared to normal controls. Thus, SIRT1 may act as a tumor suppressor through its role in DNA damage response and genome integrity.

INTRODUCTION

In *Saccharomyces cerevisiae*, Sir2 maintains genomic integrity in multiple ways. As a NAD$^+$-dependent histone deacetylase, Sir2 has been reported to regulate chromatin silencing (Blander and Guarente, 2004; Guarente, 2000). Sir2 is required for establishment and maintenance of telomeric heterochromatin (Denu, 2003; Gasser and Cockell, 2001). When overexpressed, Sir2 has been shown to extend life span in both budding yeast and *Drosophila* (reviewed in Blander and Guarente, 2004; Saunders and Verdin, 2007). Previous reports have also demonstrated that Sir2 is involved in DNA damage repair (McAinsh et al., 1999; Mills et al., 1999; Tsukamoto et al., 1997). A protein complex containing Sir2 has been reported to translocate to DNA double-strand breaks (McAinsh et al., 1999; Mills et al., 1999; Tsukamoto et al., 1997). In addition, Sir2-deficient yeast strains display defects in the nonhomologous end-joining (NHEJ) pathway of DNA double-strand break repair (Guarente, 2000).

The mammalian sirtuin family consists of seven NAD$^+$-dependent type III histone and protein deacetylases (SIRT1–7). These proteins share a catalytic domain of about 275 amino acids and are primarily localized in the nucleus (SIRT1, 6, and 7), mitochondria (SIRT3, 4, and 5), and cytoplasm (SIRT2), respectively (reviewed in Blander and Guarente, 2004; Saunders and Verdin, 2007). It has been shown that SIRT2 plays a role in the mitotic checkpoint to arrest cells if DNA damage is detected. SIRT3 enhances acetyl-CoA production by deacetylating acetyl-CoA synthetase 2. SIRT4 represses glutamate dehydrogenase to suppress insulin signaling through its ADP-ribosylase activity. SIRT6 has both ADP-ribosylase and deacetylase activity and plays a role in base excision repair. SIRT7 is involved in transcription of rRNA genes through its interaction with RNA polymerase I

SIGNIFICANCE

SIRT1 has diverse roles in various biological processes, including caloric restriction, which causes changes in glucose metabolism and life span. The role of SIRT1 in cancer is currently under debate due to recent discrepant findings. It is known that caloric restriction, which activates SIRT1, extends life span and inhibits tumorigenesis. On the other hand, SIRT1 deacetylates p53 to decrease its activity. It has therefore been hypothesized that increased SIRT1 activity, although it extends life span, may elevate cancer risk. Here we demonstrate that SIRT1 plays an important role in DNA damage response and genome integrity by maintaining proper chromatin structure and DNA damage repair foci formation. We further show that SIRT1 serves as a tumor suppressor in mice and in some types of human cancers.

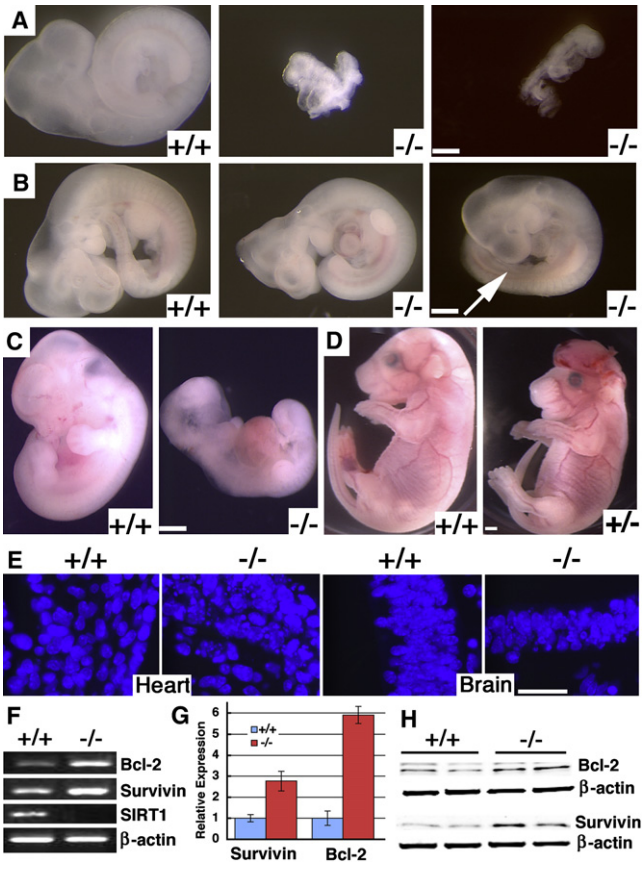

Figure 1. Deletion of SIRT1 Results in Embryonic Lethality

(A) E9.5 wild-type (+/+) and SIRT1 null (−/−) embryos. Both mutant embryos are arrested at early E8, and one (middle) has not finished turning yet.

(B) E11.25 +/+ and −/− embryos. Both −/− embryos are smaller, with abnormal shape of the head or lack of hindlimb bud (arrow).

(C) E12.5 +/+ and −/− embryos.

(D) E18.5 +/+ and +/− embryos.

(E) DAPI staining of heart and brain histological sections of E11.5 +/+ and −/− embryos.

(F–H) Expression of Bcl-2 and survivin in E11.5 +/+ and −/− embryos revealed by standard PCR (F), real-time RT-PCR (average ± SD) (G), and western blot analysis (H).

Scale bars = 500 μm in (A)–(D) and 50 μm in (E).

(reviewed in Baur et al., 2006; Haigis and Guarente, 2006; Saunders and Verdin, 2007; Vaquero et al., 2007). The most extensive study, however, has been directed toward the functions of SIRT1, the founding member of this sirtuin family and the mammalian ortholog of yeast Sir2. SIRT1 modifies histones through deacetylation of K9 in histone H3 (H3K9) and K16 in histone H4 (H4K16) and also deacetylates many nonhistone proteins that are involved in cell growth, apoptosis, neuronal protection, adaptation to caloric restriction, organ metabolism and function, cellular senescence, and tumorigenesis (Baur et al., 2006; Haigis and Guarente, 2006; Saunders and Verdin, 2007; Vaquero et al., 2007). One of the most notable targets of SIRT1 is p53, which plays a critical role in cell-cycle checkpoint regulation, apoptosis, and tumor suppression. It has been shown that overexpression of SIRT1 deacetylates p53, leading to the suppression of p53 activity (Chen et al., 2005; Kim et al., 2008; Zhao et al., 2008).

Functions of SIRT1 have also been studied at the whole-organism level using targeted gene disruption. However, SIRT1 mutant mice generated by different targeting strategies exhibit distinct phenotypes (Cheng et al., 2003). Approximately 50% of mice carrying a truncation mutation through a targeted replacement of exons 5 and 6 with a hygromycin gene died at early postnatal stages, while the remaining mice were smaller but survived to adulthood (McBurney et al., 2003). No global defects in gene silencing in these mutant mice were detected (McBurney et al., 2003). On the other hand, the majority (90%) of SIRT1 mutant animals carrying a deletion of exon 4 died perinatally, exhibiting developmental defects of the retina and heart, and the remaining 10% of these mutants were still surviving at weaning (Cheng et al., 2003). Because SIRT1 mutant cells in these animals displayed p53 hyperacetylation upon DNA damage and increased ionizing radiation-induced apoptosis in thymocytes, it was suspected that the SIRT1 deficiency might activate p53, leading to the lethality of mutant mice (Cheng et al., 2003). While these studies revealed involvement of SIRT1 in mammalian development, they were not able to recapitulate yeast Sir2 functions in gene silencing, DNA damage repair, and longevity. Of note, the role of SIRT1 in tumorigenesis is currently under debate due to some recent discrepancies. For example, the observation that SIRT1 deacetylates p53 to decrease its activity has led to the hypothesis that increased SIRT1 activity may elevate cancer risk in mammals (Chen et al., 2005). On the other hand, it was recently demonstrated that increased expression of SIRT1 reduces colon cancer formation in the $APC^{min/+}$ mouse model (Firestein et al., 2008). Furthermore, resveratrol, which activates SIRT1 (Howitz et al., 2003), exhibits chemopreventive activity against various cancers including leukemia (Li et al., 2007), DMBA-induced mammary tumors in rats (Whitsett et al., 2006), skin cancer (Aziz et al., 2005), and prostate cancer (Harper et al., 2007).

In this study, we created a SIRT1 mutant mouse model and studied the role of SIRT1 in DNA damage response and tumorigenesis. Our data provide strong evidence that mammalian SIRT1 plays an important role in DNA damage repair, genomic integrity, and inhibition of tumorigenesis.

RESULTS

Generation of SIRT1 Mutant Mice

The *Sirt1* gene was mutated by deleting exons 5 and 6, which encode a part of the catalytic domain (see Figures S1A–S1D available online). Western blot analysis using an antibody to the N terminus of SIRT1 revealed that there was no truncated protein in embryos homozygous for the mutation (Figure S1D), suggesting that the SIRT1 mutation we created is a candidate null mutation.

Previous investigations showed that mice carrying mutations of SIRT1 died at perinatal stages up to several months into adulthood (Cheng et al., 2003; McBurney et al., 2003). However, we found that embryos homozygous for the mutation ($Sirt1^{-/-}$) began to die at embryonic day 9.5 (E9.5) (Figure 1A; Table S1). Abnormal $Sirt1^{-/-}$ embryos were also found at later stages of development (Figures 1B and 1C). There was a significant decrease in $Sirt1^{-/-}$ embryos at E14.5–E16.5, and no homozygous embryos were found at E17.5–E18.5 among

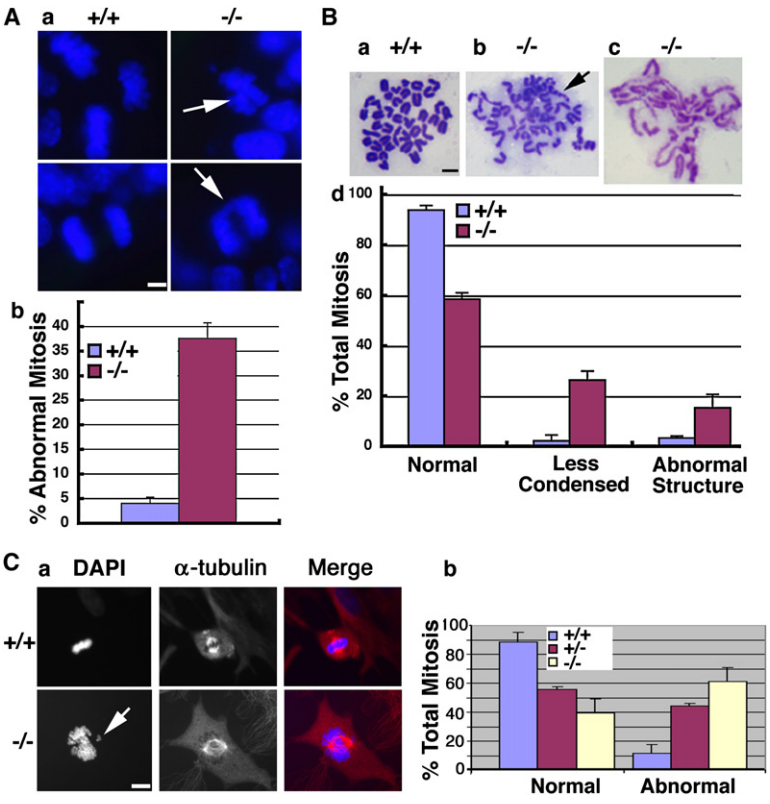

Figure 2. Deletion of SIRT1 Causes Chromosome Abnormality

(Aa) DAPI staining of tissue sections showing abnormal mitotic features in an E10.5 *Sirt1*$^{-/-}$ embryo.

(Ab) Data were collected from three pairs of embryos; 200 mitotic phases from each embryo were counted.

(Ba–Bc) Chromosome spreads from E9.5 embryos showing normal spread (Ba), aneuploid and abnormal structures or broken chromosomes (arrow, Bb), and less condensed chromosomes (Bc).

(Bd) Chromosome spreads from nine pairs of embryos were prepared, and all of the spreads from each individual embryo were counted.

(Ca) SIRT1 mutant MEFs display incompletely condensed and lagging chromosomes (arrow) and uneven chromosome segregation under a relative normal spindle (α-tubulin staining).

(Cb) Summary of data from (Ca).

Data are presented as average ± SD. Scale bars = 10 μm in (A) and (B) and 20 μm in (C).

69 embryos dissected. Some *Sirt1*$^{+/-}$ embryos also exhibited exencephaly (Figure 1D). After analyzing 442 offspring, we found that the survival rate of homozygous SIRT1 mutant mice was about 1% in a 129SvEv/FVB background and 9.3% in a 129SvEv/FVB/Black Swiss background (Table S1). These observations indicated that our *Sirt1*$^{-/-}$ mice exhibited more severe phenotypes than those reported previously (Cheng et al., 2003; McBurney et al., 2003).

SIRT1 Deficiency Results in Accumulation of Cells in the Early Phase of Mitosis

In order to understand the phenotype, we further analyzed *Sirt1*$^{-/-}$ mice during embryonic development. Most E10.5–E12.5 *Sirt1*$^{-/-}$ embryos were abnormally small, and DAPI staining showed nuclear fragmentation and cell death (Figure 1E). However, these dead cells were negative for TUNEL assay, suggesting that the cell death might not be caused by typical apoptosis. Further analysis of the embryos demonstrated that some antiapoptotic genes, such as *Bcl-2* and *survivin*, were elevated in SIRT1 null embryos (Figures 1F–1H), which might protect *Sirt1*$^{-/-}$ cells from apoptosis. We next analyzed cell proliferation using BrdU labeling (Figures S2A–S2C) and phosphorylated histone H3 staining, a marker for cells at the early phase of mitosis (Figures S2D–S2F). *Sirt1*$^{-/-}$ embryos had 15%–20% more BrdU labeling at E10.5 and E11.5 than control embryos, but the labeling returned to normal levels at E12.5 (Figure S2C). During the same time period, *Sirt1*$^{-/-}$ embryos had 1.5- to 2-fold more cells that were positive for phosphorylated histone H3 compared to wild-type controls (Figure S2F). Histone H3 phosphorylation occurs in prophase, which is normally for a short duration. The marked increase of phosphorylated histone H3 suggests that SIRT1 deficiency causes abnormal accumulation of cells in the early phases of mitosis.

SIRT1 Deficiency Causes Incomplete Chromosome Condensation and Chromosome Instability

To investigate this further, we examined mitotic chromosome morphology in the embryos. Staining tissue sections of E10.5 embryos with DAPI indicated that *Sirt1*$^{-/-}$ embryos exhibited chromosome abnormalities characterized by chromosome lagging and unequal segregation (Figure 2A). These abnormal chromosome structures were found in 37% of *Sirt1*$^{-/-}$ cells, compared with less than 5% of wild-type cells. Chromosome spreads prepared from E9.5 embryos showed that about 37% of *Sirt1*$^{-/-}$ cells were aneuploid and displayed a variety of structural aberrations, such as broken and decondensed chromosomes (Figure 2B). Analysis of chromosome spreads prepared from *Sirt1*$^{-/-}$ mouse embryonic fibroblasts (MEFs) detected similar abnormalities (data not shown). Next, we analyzed metaphase chromosomes in cells that were not treated with colcemid using an antibody against α-tubulin together with DAPI staining. In wild-type cells, chromosomes at metaphase are highly condensed and aligned along with the metaphase plate. However, many *Sirt1*$^{-/-}$ MEFs at metaphase contained a partially condensed and disorganized chromosomal mass that was associated with a relatively normal spindle (Figure 2C). Chromosome aneuploidy and breaks could conceivably originate from the continuous division of these mutant cells.

SIRT1 Deficiency Impairs Heterochromatin Formation

It is known that SIRT1 deacetylates K16 of histone H4 and K9 of histone H3 in yeast and in in vitro-cultured mammalian cells (Vaquero et al., 2007). Western blotting with antibodies against Ac-K9 and Ac-K16 revealed increased levels of both H3 Ac-K9 and H4 Ac-K16 in *Sirt1*$^{-/-}$ MEFs (Figures 3A and 3B), and reconstitution of SIRT1 in these cells reduced their acetylation (Figure 3C). Because histone acetylation plays a major role in chromosome condensation, we hypothesized that the alteration

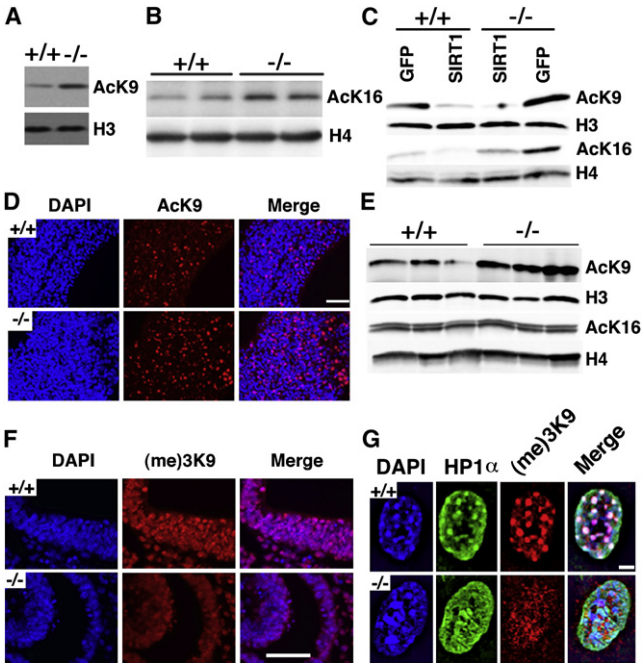

Figure 3. SIRT1 Deficiency Alters Epigenetic Modification of Chromatin

(A and B) Western blot analysis showing increased histone H3K9 (A) and H4K16 (B) levels in *Sirt1*$^{-/-}$ (−/−) MEFs.

(C) Reconstitution of SIRT1 in −/− MEFs reduces histone Ac-K9 and Ac-K16 levels.

(D and E) Ac-K9 immunofluorescence staining of brain in E11 embryos (D). −/− embryos displayed much more Ac-K9 staining than +/+ embryos, which is confirmed by western blot analysis (E).

(F) (me)3-K9 immunofluorescence staining of E11 brain. −/− embryos display much less (me)3-K9 staining than +/+ embryos.

(G) In MEFs, loss of SIRT1 impairs distribution of HP1α. Deletion of SIRT1 causes diffused localization compared with punctuated foci in +/+ embryos. Scale bars = 100 μm in (D) and (F) and 10 μm in (G).

in histone modification in *Sirt1*$^{-/-}$ embryos might be a cause of the chromosomal abnormalities. To investigate this, we performed immunofluorescence staining on brain sections of E11 embryos. Our data showed that SIRT1 mutants contained a much higher level of H3 Ac-K9 (Figure 3D), while no significant alteration of H4 Ac-K16 was detected (data not shown). This finding was confirmed by western blot analysis (Figure 3E), demonstrating that mammalian SIRT1 is capable of modifying histones in vivo, although in the early embryos, SIRT1 seemed to have stronger effects on acetylation of histone H3K9 than histone H4K16.

Increased acetylation of K9 on histones impairs its trimethylation level, thus affecting heterochromatin formation. To verify this point, an antibody against trimethylated K9 ((me)3-K9) was applied to brain sections from E11 embryos (Figure 3F). *Sirt1*$^{-/-}$ mutant brain contained much less trimethylated K9 than control brain. Similarly, a distinct reduction in trimethylated K9 foci was also detected in *Sirt1*$^{-/-}$ MEFs (Figure 3G). A function of trimethylated K9 is to recruit heterochromatin protein 1 (HP1α). HP1α contains a chromatin modification organizer motif that binds to histone methyltransferases in order to establish a closed chromatin configuration that represses transcription. We did not detect distinct HP1α foci in *Sirt1*$^{-/-}$ cells although HP1α was diffusely present, and consequently, there was no colocalization between trimethylated K9 and HP1α. The impaired heterochromatin formation accounts for reduced chromosome condensation, which could be a cause of genomic instability.

SIRT1 Deficiency Results in Cell-Cycle Abnormalities and Impaired DNA Damage Repair

Genetic instability could also result from cell-cycle checkpoint defects and impaired DNA damage repair (Deng, 2006). To comprehensively understand the effect of SIRT1 deficiency, we studied cell-cycle checkpoints and DNA damage repair. Our analysis failed to detect obvious abnormalities in the G2/M cell-cycle checkpoint in *Sirt1*$^{-/-}$ cells (data not shown). When cells were treated with 10 Gy of γ irradiation (IR), both wild-type (WT) and *Sirt1*$^{-/-}$ MEFs showed a similar reduction (~60%) of cells in S phase, suggesting that *Sirt1*$^{-/-}$ cells have a normal G1/S cell-cycle checkpoint (Figure 4A). However, we found that *Sirt1*$^{-/-}$ MEFs did not respond to lower doses of γ irradiation (Figure 4B), revealing G1/S checkpoint defects under these conditions. Thus, the large-scale DNA damage induced by a high dose of IR is sufficient to activate redundant checkpoint signaling cascades in *Sirt1*$^{-/-}$ cells. Of note, H2AX mutant and Nijmegen breakage syndrome (NBS) mutant cells showed a similar response, i.e., exhibiting G1/S and/or G2/M defects at low but not high doses of IR (Antoccia et al., 1997; Ferguson and Alt, 2001).

Next, we assessed DNA damage repair ability in *Sirt1*$^{-/-}$ cells. To investigate this, MEFs were transfected with a microhomologous DNA damage repair reporter, the pGL2-Luc vector, linearized with either HindIII or EcoRI. Forty-eight hours post-transfection, the cells were collected and luciferase activity was quantified. With HindIII digestion, there was no significant difference in Luc activity between wild-type and *Sirt1*$^{-/-}$ cells. In contrast, upon EcoRI digestion, the wild-type cells were able to recover about 70% of Luc activity while *Sirt1*$^{-/-}$ cells recovered only 42% (Figure 4C). Because EcoRI cuts within the coding sequence of the luciferase gene, the restoration of luciferase activity therefore requires the precise rejoining of the short protruding ends, which involves microhomologous DNA damage repair. The reduced Luc activity in SIRT1 mutant cells indicates that the absence of SIRT1 reduces the microhomologous DNA damage repair ability. On the other hand, because HindIII cuts within the linker region between the SV40 promoter and the Luc coding sequence, the restoration of luciferase activity does not require precise end joining. These data indicate that the absence of SIRT1 does not interfere with end ligation if such a ligation does not require a precise end rejoining.

To further illustrate the effect of impaired DNA damage repair, we used the comet assay, an extremely sensitive assay to detect DNA damage at the single-cell level. We found that *Sirt1*$^{-/-}$ cells contained, on average, an ~2-fold longer comet tail (12.44 μM) than wild-type cells (6.74 μM) when quantitatively measured 2 hr post 5 Gy γ irradiation (Figures 4D and 4E). We also performed a radiosensitivity assay using a serially increased dosage of γ irradiation (Figure 4F). We found that *Sirt1*$^{-/-}$ cells were significantly more sensitive to radioactivity compared to wild-type cells at doses up to 5 Gy. These data are consistent with the finding that *Sirt1*$^{-/-}$ cells have impaired DNA damage repair. Because γ irradiation primarily causes DNA double-strand breaks,

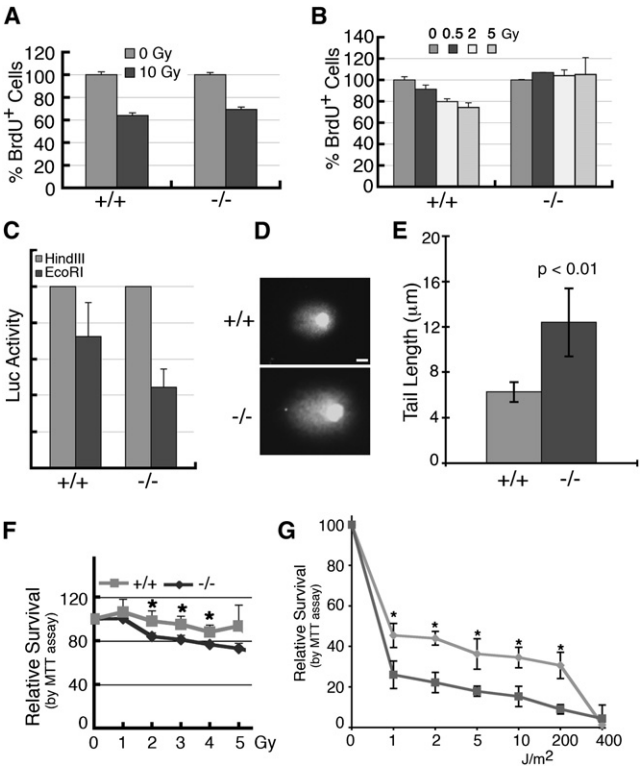

Figure 4. Deletion of SIRT1 Leads to Impaired DNA Damage Repair and Radiation Sensitivity

(A and B) SIRT1 deletion caused impaired response to a low dosage of γ irradiation (B), but not to high dosage (A), when assessed by BrdU incorporation 24 hr after irradiation.

(C) SIRT1 mutant cells exhibit impaired microhomologous recombination as revealed in cells transfected with a pGL2-Luc vector that was linearized with either HindIII or EcoRI.

(D and E) Comet assay reveals that *Sirt1*$^{-/-}$ (−/−) cells are incapable of efficiently repairing γ irradiation-induced double-strand DNA damage. Comet assay was performed 2 hr after MEFs received 5 Gy of γ irradiation. Scale bar in (D) = 100 μm.

(F and G) −/− MEFs are more sensitive than +/+ controls as revealed by γ irradiation (F) and ultraviolet radiation (G). *$p < 0.05$.

All data were obtained by analyzing at least six pairs of individual MEFs at passage 1. Data are presented as average ± SD.

we also treated cells with ultraviolet (UV) radiation, which induces single-strand breaks. We found that *Sirt1*$^{-/-}$ cells were also more sensitive to UV radiation than wild-type cells (Figure 4G), suggesting that SIRT1 may be also involved in other types of DNA damage repair, such as base excision repair.

Defective DNA Damage Repair Correlates with Decreased γH2AX Foci Formation

To investigate the mechanistic base of impaired DNA damage repair, we stained the cells with an antibody to γH2AX, which is a DNA damage sensor and helps maintain genome integrity (Celeste et al., 2003). Upon γ irradiation, *Sirt1*$^{-/-}$ cells showed markedly decreased γH2AX foci compared with WT cells (Figure 5A). There are at least two possible factors resulting in a decrease in γH2AX foci formation: lack of initial phosphorylation or lack of retention of phosphorylation. To distinguish between these possibilities, we irradiated MEFs with 3 Gy IR and then followed γH2AX foci formation during a time course. We found that the initial γH2AX foci were significantly fewer in *Sirt1*$^{-/-}$ MEFs (20 foci/cell) than in WT cells (48 foci/cell). After 15 min of IR, both *Sirt1*$^{-/-}$ and WT cells maintained a similar increase at 30 and 60 min after treatment (Figure 5B). This observation indicates that SIRT1 deficiency reduces initial H2AX phosphorylation while the ability of retaining H2AX phosphorylation is not affected. The differential levels of γH2AX were also detected by western blot analysis (Figure 5C). To confirm this, we treated WT cells with trichostatin A (TSA, an inhibitor of class I and II histone deacetylases) and/or nicotinamide (NIC, an inhibitor of class III histone deacetylases) followed by western blot with an antibody to γH2AX. These data confirmed that the inhibition of class III, but not class I and II, histone deacetylases inhibited H2AX phosphorylation (Figure 5D). Indeed, inhibition of class I and II histone deacetylases increased levels of γH2AX, even in the presence of nicotinamide. These data suggest that class I/II and class III histone deacetylases have opposing roles in H2AX phosphorylation and that the negative effect of class I/II histone deacetylases could supersede the positive effect of class III histone deacetylases if both deacetylases are inhibited.

To assess whether the reduced γH2AX foci formation is a direct consequence of SIRT1 loss, we transfected *Sirt1*$^{-/-}$ cells with a SIRT1 expression vector. Our data indicated that the SIRT1-reconstituted *Sirt1*$^{-/-}$ cells contained relatively equal numbers of γH2AX foci compared with WT controls upon 3 Gy treatment (Figure 5E). Since γH2AX foci formation serves as a sensor for DNA damage (Kobayashi, 2004; Paull et al., 2000), impairment at this step may affect the downstream response to DNA damage. To investigate this, we examined foci formation of Rad51, BRCA1, and NBS1 following γ irradiation. Our data revealed marked reduction in nuclear foci formation of these proteins in SIRT1 mutant mice compared with WT MEFs (Figures 5F–5H). Of note, our western blot analysis did not reveal changes in protein levels (Figure 5I), suggesting that these proteins cannot be efficiently recruited to DNA damage sites in SIRT1 mutant cells.

H2AX can be phosphorylated by ataxia telangiectasia mutated (ATM) upon γ irradiation. Therefore, we studied ATM phosphorylation and its downstream substrates. Immunofluorescence staining with an antibody to phosphorylated ATM (pi-ATM) did not reveal significant changes in pi-ATM foci in *Sirt1*$^{-/-}$ MEFs post γ irradiation (Figure S3A). Western blots showed that after γ irradiation, levels of phosphorylated CHK2 and p53(Ser20) showed no obvious difference between WT and *Sirt1*$^{-/-}$ MEFs (Figures S3B and S3C). Altogether, these observations suggest that SIRT1 deficiency impairs DNA damage response and that this effect is independent of the ATM/CHK2/p53 pathway.

Haploinsufficiency of SIRT1 Facilitates Tumorigenesis

Genetic instability is a major cause of tumor formation (Deng, 2001). However, a role of SIRT1 in tumorigenesis could not be determined due to embryonic lethality. Since the absence of SIRT1 increases p53 activity, it has been suspected that embryonic lethality of SIRT1 mutant embryos is due at least in part to p53 activation (Cheng et al., 2003). To test this, we introduced a p53 null mutation into SIRT1 mutant mice. We failed to obtain *Sirt1*$^{-/-}$;*p53*$^{-/-}$ mice among 429 pups generated from interbreeding between *Sirt1*$^{+/-}$;*p53*$^{+/-}$ mice, although five

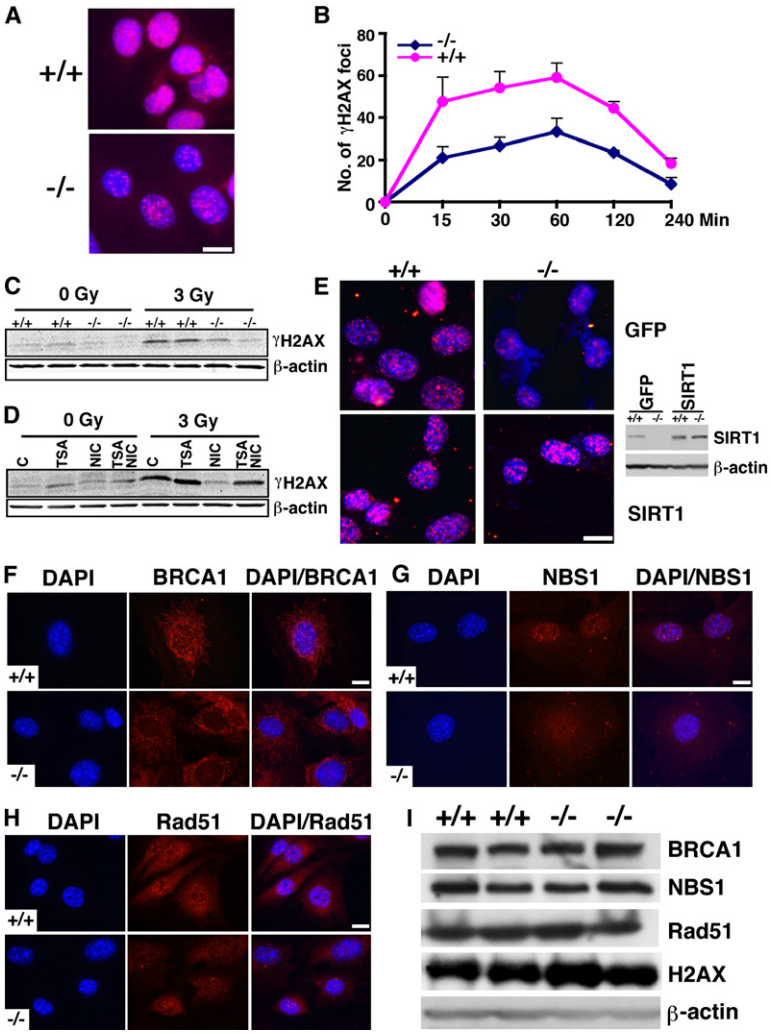

Figure 5. SIRT1 Deficiency Impairs γH2AX Foci Formation

(A) γH2AX foci formation is reduced 2 hr after 3 Gy irradiation.

(B) Time course showing reduced initiation of γH2AX foci in SIRT1 mutant cells. Six pairs of MEFs at passage 1 were irradiated with 3 Gy, and γH2AX foci number was counted in each individual cell. One hundred of each type of MEF were counted in both untreated and 3 Gy-irradiated cells. *$p < 0.05$. Data are presented as average ± SD.

(C) Western blot showing significantly reduced γH2AX levels in *Sirt1*$^{-/-}$ (−/−) compared to +/+ cells.

(D) Nicotinamide (NIC) treatment diminished γH2AX levels in *Sirt1*$^{+/+}$ cells.

(E) Transfection of a vector carrying wild-type SIRT1 (pUSE-SIRT1, Upstate), but not a GFP control, restored γH2AX foci formation in −/− cells. SIRT1 expression levels by western blot analysis are shown at right.

(F–H) Immunofluorescence staining of BRCA1 (F), NBS1 (G), and Rad51 (H) in +/+ versus −/− MEFs. Nuclear foci formation is reduced in the mutant cells.

(I) Western blots showing no alteration in total protein levels of BRCA1, NBS1, Rad51, and H2AX.

Scale bars = 100 μm in (A) and (E) and 10 μm in (F)–(H).

(5/429 = 1.2%) *Sirt1*$^{-/-}$;*p53*$^{+/-}$ mice were obtained (Table S2). Thus, absence of p53 did not rescue the embryonic lethality associated with SIRT1 deficiency, suggesting that the embryonic lethality associated with SIRT1 deficiency is not caused by p53 activation.

Sirt1$^{+/-}$;*p53*$^{+/-}$ mice were healthy; however, they started to develop spontaneous tumors from about 5 months of age, and tumor incidence reached about 76% by 20 months of age, while only 2 out of 21 *Sirt1*$^{+/-}$ mice and 3 out of 22 *p53*$^{+/-}$ mice developed tumors during the same period of time (Figure 6A). The tumors that occurred in *Sirt1*$^{+/-}$;*p53*$^{+/-}$ mice were primarily sarcomas (45.9%), lymphomas (35%), teratomas (21.6%), and carcinomas (16.2%) (Figure 6B; Figure S4). Chromosome spreads from primary tumors (11 tumors) showed extensive aneuploidy (83.8%) and chromosomal aberrations, notably translocations, chromosome breaks, deletions, and dicentric chromosomes (Figure 6C).

Spectral karyotyping (SKY) analysis was performed on metaphase spreads derived from early passages of two primary tumors, 841A (mammary gland carcinoma) and 785S (hemangiosarcoma) (Figure 6D). SKY analyses on metaphase spreads derived from primary cells at early passages of tumor 785S showed a variety of clonal aberrations. The nonreciprocal translocation involved chromosome 13 and chromosome 2, giving rise to a T(13;2) translocation (30%), and a complex translocation involving an insertion of chromosome 4 into chromosome 10 resulted in a T(10;4;10) translocation or T(4;10) (30%) (Figure 6D; Figure S5A). Dicentric chromosomes were observed involving two copies of chromosome 6 in a Dic(6;6) (40%) (Figure 6D; Figure S5B). Numerous chromosome breaks producing both acentric and centric chromosome fragments from chromosomes 1, 2, 4, 8, 10, and 19 were identified (Figure 6D). Furthermore, 50% of the spreads lost chromosome 10, 70% lost chromosome 7, and 60% lost chromosome 12. Extensive chromosome abnormality was observed in cells from 841A carcinomas (Figure S5A). All of these clonal aberrations recorded from 841A and 785S metaphase spreads were confirmed by fluorescence in situ hybridization (FISH) (Figures S5B–S5E). Both of these tumors showed random gains and losses of whole chromosomes. However, a consistent and recurrent gain of chromosome 3 (>90%) and loss of chromosome 7 (55%) was observed in spreads from both tumors. Taken together, these results demonstrate that SIRT1 deficiency severely impairs genome integrity and/or stability and could be one of the causes for spontaneous tumorigenesis in *Sirt1* and *p53* double-heterozygous animals.

RT-PCR analysis of tumor tissues demonstrated that 73% (11 of 15) of the tumors examined lost p53 expression and 27% (4 of 15) of the tumors lost SIRT1 expression (Figure S6A). Southern blot showed that 77% (10 of 13) exhibited loss of heterozygosity (LOH) of *p53* (Figure S6B). Next, we examined SIRT1 protein levels in tumor tissues by western blot analysis and found that 44% (7 of 16) of the tumors had no or low levels of SIRT1 (Figure S6C). Meanwhile, Southern blot analysis revealed that 18% (3 of 17) of the tumors showed LOH of *Sirt1* (Figure S6D).

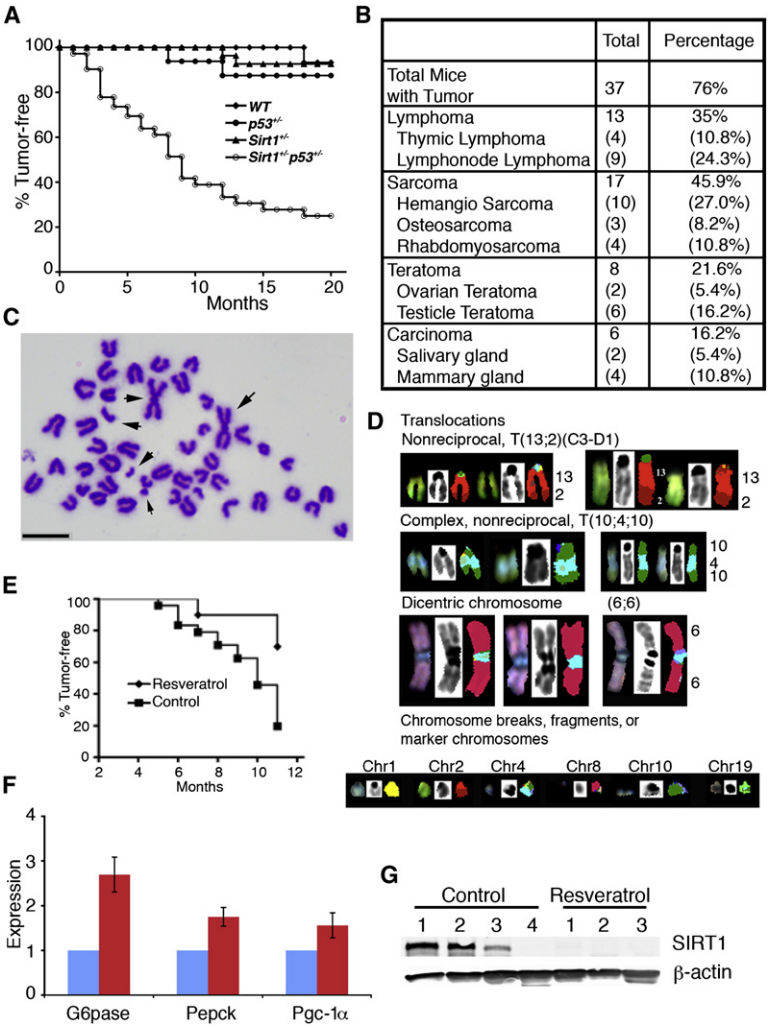

	Total	Percentage
Total Mice with Tumor	37	76%
Lymphoma	13	35%
Thymic Lymphoma	(4)	(10.8%)
Lymphonode Lymphoma	(9)	(24.3%)
Sarcoma	17	45.9%
Hemangio Sarcoma	(10)	(27.0%)
Osteosarcoma	(3)	(8.2%)
Rhabdomyosarcoma	(4)	(10.8%)
Teratoma	8	21.6%
Ovarian Teratoma	(2)	(5.4%)
Testicle Teratoma	(6)	(16.2%)
Carcinoma	6	16.2%
Salivary gland	(2)	(5.4%)
Mammary gland	(4)	(10.8%)

Figure 6. SIRT1 Deficiency Causes Genomic Instability and Tumor Formation

(A) Tumor-free curve of different genotypes of mice, including WT (n = 18), $p53^{+/-}$ (n = 12), $Sirt1^{+/-}$ (n = 37), and $Sirt1^{+/-};p53^{+/-}$ (n = 49).

(B) Types and percentages of tumors developed in $Sirt1^{+/-};p53^{+/-}$ mice.

(C) Chromosome spread from a mammary tumor. Regardless of the tumor type, general events observed include aneuploidy, numerous structural chromosomal aberrations, and premature chromosome segregation. Arrows point to abnormal chromosomes. Scale bar = 10 μm.

(D) Spectral karyotyping (SKY) analysis of metaphase spreads from a primary tumor showing nonreciprocal translocation (T(13;2)(C3-D1)), complex nonreciprocal translocation (T(10;4;10)), dicentric chromosomes, and a variety of chromosomal fragments from chromosomes 1, 2, 4, 8, 10, and 19, respectively.

(E) Resveratrol treatment reduces tumor incidence in $Sirt1^{+/-};p53^{+/-}$ mice. The resveratrol-treated group consisted of 10 female mice. The control group contained 10 DMSO-treated and 16 untreated female mice. Log rank test: $p < 0.01$.

(F) Resveratrol treatment causes altered expression of several known downstream genes of SIRT1. Data are presented as average ± SD.

(G) Western blot analysis showing that all three tumors developed in the resveratrol-treated $Sirt1^{+/-};p53^{+/-}$ mice lost SIRT1 expression, while only one out of four tumors in the mock-treated mice lost SIRT1 expression.

The observation that the majority of tumors maintained one wild-type allele of *Sirt1* suggests that SIRT1 serves as a haploid tumor suppressor gene. To test this, we investigated whether this *Sirt1* allele is functional by using resveratrol, an activator of SIRT1 (Howitz et al., 2003). Female $Sirt1^{+/-};p53^{+/-}$ mice were randomized into two groups. One group (n = 10) was provided with resveratrol-supplemented drinking water (7.5 μg/ml), while the other group was provided with drinking water either with (n = 10) or without (n = 16) carrier (DMSO) supplement. The treatment started at 2 months of age and lasted for 9 months. During this period, 21 out of 26 (80%) of the mice in the control group developed tumors; in contrast, only 3 out of 10 (30%) of the mice in the resveratrol-treated group developed tumors (1 hemangiosarcoma and 2 thymic lymphomas). We noticed that the partial inhibition of tumor formation was also correlated with a delay in tumor onset, i.e., the first tumor occurred in the control group at 5 months of age, while the first tumor in the treated group occurred at 7 months of age (Figure 6E).

Next, we investigated whether the reduced tumor formation was due to SIRT1 activation. We first examined expression of several SIRT1 downstream genes, including *G6pase*, *Pepck*, and *Pgc-1α* (Lagouge et al., 2006; Rodgers et al., 2005). We detected significantly increased levels of these genes in resveratrol-treated compared with control $Sirt1^{+/-};p53^{+/-}$ mice (Figure 6F), suggesting that the remaining copy of *Sirt1* in $Sirt1^{+/-};p53^{+/-}$ mice is activated. We showed earlier that 18% of tumors exhibited LOH of *Sirt1* and up to 44% of tumors had no or low levels of SIRT1. Resveratrol should not inhibit growth of tumors if they are negative for SIRT1. To see if this was the case, we performed western blot analysis for SIRT1 expression in these tumors. We found that one of four tumors developed in the DMSO-treated group lost SIRT1 protein, while all three tumors developed in resveratrol-treated mice did not contain SIRT1 protein (Figure 6G). The loss of SIRT1 in these tumors explains why resveratrol did not inhibit their formation. However, the cause for the loss of SIRT1 protein in these tumors remains elusive, as no LOH of *Sirt1* was detected by Southern blot analysis (Figure S6E).

Expression Levels of SIRT1 in Clinical Cancer Samples

Our view that SIRT1 may serve as a tumor suppressor seems, at least on the surface, contradictory to current reports that SIRT1 is expressed in certain primary tumors and cell lines at high levels. This includes prostate cancer (Huffman et al., 2007), acute myeloid leukemia (Bradbury et al., 2005), nonmelanoma skin cancers (Hida et al., 2007), and colon cancer (Stunkel et al., 2007). To investigate this, we compared SIRT1 levels in the available data sets; surprisingly, we found that SIRT1 levels are actually lower in many cancers than normal tissues, including glioblastoma, bladder carcinoma, prostate carcinoma, and various forms of ovarian cancers (Figure S7). To provide our own assessment for this issue, we performed the following three experiments.

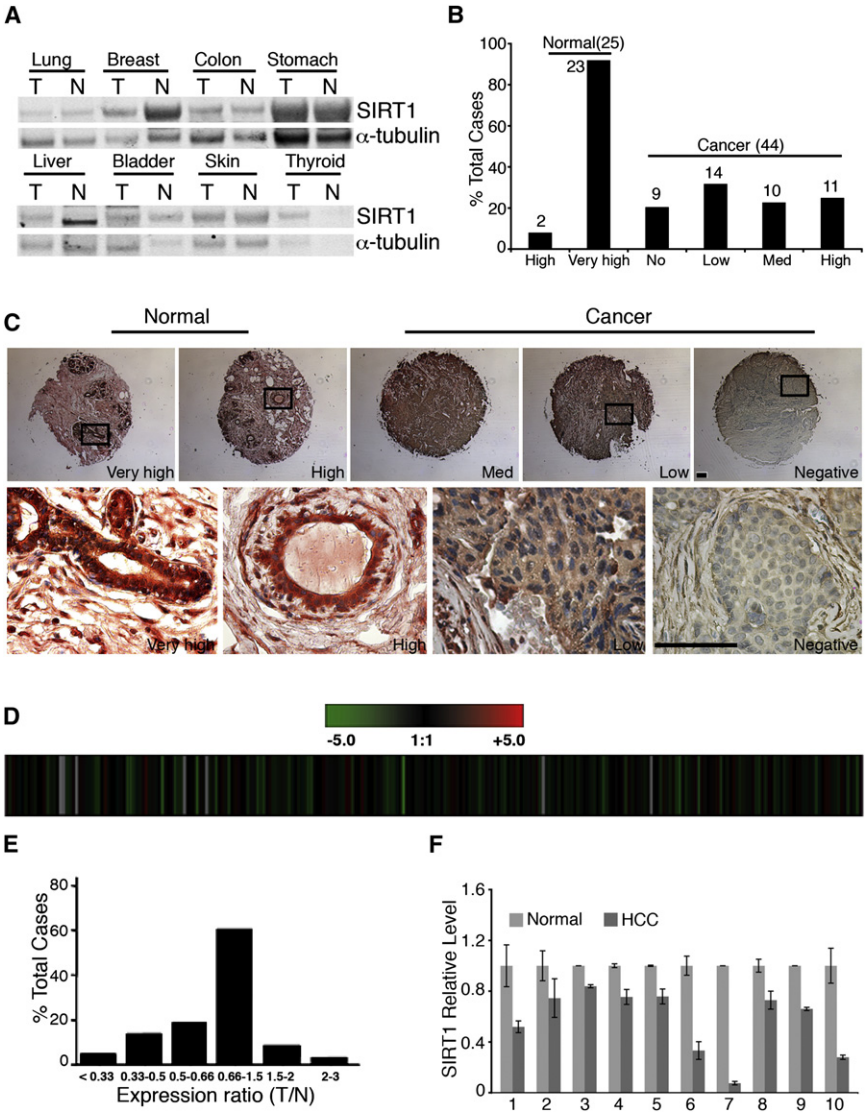

Figure 7. *SIRT1* Gene Expression in Human Clinical Cancers

(A) Levels of SIRT1 in eight different cancers and their normal controls measured by western blot analysis.

(B and C) SIRT1 protein levels in 44 breast cancers and 25 normal breast tissue samples measured by tissue array.

(B) Levels of SIRT1 staining were classified as negative (No), low, medium, high, or very high.

(C) Immunohistochemical images. The boxed regions (enlarged below) show high levels of SIRT1 in normal epithelium and lowered levels in cancers. Scale bars = 100 μm.

(D) SIRT1 expression levels in microarray data from 263 hepatic cell carcinoma (HCC) samples, presented as raw log2 ratio of tumors to paired noncancerous liver tissues (T/N) using a previously described data set (GEO accession number GSE5975) (Yamashita et al., 2008). Each bar represents an individual case, and pseudocolors indicate transcript levels below, equal to, or above the mean (green, black, and red, respectively). Missing data are denoted in gray. The scale represents the gene expression ratios from −5 to +5 in log2 scale.

(E) HCC cases categorized by relative SIRT1 expression levels based on geometric fold changes.

(F) Real-time RT-PCR data (average ± SD) from ten pairs of samples.

First, we performed western blot analysis of eight types of tumors, including lung, breast, colon, stomach, liver, bladder, skin, and thyroid. Our data revealed reduced SIRT1 levels in breast cancer and hepatic cell carcinoma (HCC) compared to their normal controls, while slightly increased (thyroid) or unchanged (lung, colon, stomach, bladder, and skin) SIRT1 levels were detected in other tumors (Figure 7A). Next, we performed tissue array analysis to compare SIRT1 protein levels between 44 breast cancers and 25 normal breast tissue samples. Our data detected significantly higher levels of SIRT1 in all normal breast tissue samples than in cancers (Figures 7B and 7C). We also analyzed *SIRT1* expression levels in microarray data from 263 HCC samples. Our data indicated that *SIRT1* was reduced 2-fold in 42 of 263 tumors, increased 2-fold in 4 tumors, and unchanged in the remaining 217 tumors (Figures 7D and 7E). To provide a validation of the microarray data, we randomly picked 10 HCC samples that showed reduced levels of SIRT1 and performed real-time RT-PCR on these samples. Our data revealed reduction of SIRT1 in all of the samples compared with their normal controls (Figure 7F).

Altogether, the observations that $Sirt1^{+/-};p53^{+/-}$ mice develop tumors in multiple tissues and that SIRT1 levels are reduced in many human cancers provide strong evidence that SIRT1 may function as a tumor suppressor in mice and in some human tissues.

DISCUSSION

We have shown that the majority of our $Sirt1^{-/-}$ mice died at E9.5–E14.5. This phenotype is more severe than that of the other two SIRT1 mutant mice reported previously (Cheng et al., 2003; McBurney et al., 2003). A number of possible reasons could account for this difference. First, all of these mutant mice were studied in different genetic backgrounds. The mice used by McBurney et al. (2003) were generated using R1 embryonic stem (ES) cells derived from embryos of 129Sv × 129Sv-CP (Nagy et al., 1993). Homozygous SIRT1 mutant mice on the 129Sv-CP background were smaller and invariably died within 1 month after birth, while on the 129/CD1 mixed background, the mutants more often survived to adulthood, although their stature was smaller than that of their littermates (McBurney et al., 2003). The mice used by Cheng et al. (2003) and our mice were generated using TC1 ES cells derived from embryos of 129SvEv mice (Deng et al., 1996). On the 129SvEv/C57BL/6 background, about 90% of mutant mice died at perinatal or early postnatal stages, and most of the remaining mutant animals died about 3 months after birth (Cheng et al., 2003). In our study, the majority of the $Sirt1^{-/-}$ (deletion of exons 5 and 6) mice died at middle stages of embryonic

development, while about 1% on the 129SvEv/FVB background and 9.3% on the 129SvEv/FVB/Black Swiss background survived to adulthood. These observations indicate that the genetic background has a profound effect on the phenotypes of all three SIRT1 mutant strains. Furthermore, these mutant mice also contained distinct targeted mutations, i.e., a replacement of exons 5 and 6 with a hygromycin gene (McBurney et al., 2003), a deletion of exon 4 (Cheng et al., 2003), or a deletion of exons 5 and 6 (this study) using the Cre/loxP-mediated approach. The potential effect of these different mutations on phenotypes of SIRT1 mutant mice is currently unclear, as no truncated SIRT1 protein was observed in these mutant mice.

Absence of SIRT1 Causes Genetic Instability

What is the cause (or causes) of the early lethality of SIRT1 mutant embryos? Our data revealed several major defects that may contribute to embryonic lethality. Mutant embryos analyzed at E10.5–E12.5 exhibited an altered pattern of histone modification, i.e., reduced levels of (me)3-K9 and increased acetylation of H3K9. These data provide in vivo evidence for the function of SIRT1 in histone modification previously found in yeast and cultured cells (Vaquero et al., 2007). A consequence of altered acetylation is reduced chromosome condensation, which may account for why mutant embryos contained 1.5- to 2-fold more cells in the prophase of mitosis. In addition, we also detected loosely compacted chromosomes in the metaphase. This abnormality may interfere with normal progression of the remaining phases of mitosis and consequently lead to the formation of chromosome bridges, chromosome breaks, unequal chromosome segregation, and aneuploidy. The extensive genetic instability may be a primary reason for the death of mutant embryos.

In yeast, Sir2 plays a role in DNA damage repair (McAinsh et al., 1999; Mills et al., 1999; Tsukamoto et al., 1997). This function, however, has not been demonstrated in its mammalian homolog, SIRT1. Our study detected impaired microhomology-mediated DNA damage repair and double-strand break repair in SIRT1 mutant cells. The marked reduction of γH2AX, Rad51, BRCA1, and NBS1 foci formation upon DNA damage could serve as a cause of the reduced efficiency of DNA damage repair. Furthermore, recent studies have indicated that SIRT1 acetylates Ku70 (Jeong et al., 2007) and NBS1 (Yuan et al., 2007). All of these proteins are involved in the regulation of cellular response to DNA double-strand breaks and/or DNA damage repair, although the involvement of other factors needs to be investigated.

SIRT1 Is a Haploinsufficient Tumor Suppressor Gene

The role of SIRT1 in cancer is currently under debate. SIRT1 is overexpressed in several types of human cancers (Bradbury et al., 2005; Hida et al., 2007; Huffman et al., 2007; Stunkel et al., 2007). However, it is unclear whether SIRT1 simply serves as a marker for tumorigenesis or indeed affects tumor growth (Lim, 2006). The regulation of the cellular response to DNA damage and maintenance of genetic stability may indicate that SIRT1 inhibits tumor formation (Stunkel et al., 2007). Consistent with this, it has recently been demonstrated that increased expression of SIRT1 reduces colon cancer formation in the $APC^{min/+}$ mouse model (Firestein et al., 2008). On the other hand, data also uncover a role of SIRT1 in deacetylating p53, leading to p53 inhibition (Chen et al., 2005). More recently, it has been shown that inhibition of SIRT1 using a specific inhibitor causes p53 hyperacetylation and increases p53-dependent transcription activity (Lain et al., 2008).

On the other hand, previous studies revealed that p53 can be activated by targeted mutation of several genes, such as *Brca1* (Xu et al., 2001), leading to embryonic lethality, which can be suppressed by introduction of a p53 null mutation. Therefore, we reasoned that if the lethality of SIRT1 mutant mice is attributed to activation of p53, the simultaneous mutation of p53 should have some impact on *Sirt1* phenotypes. To test whether embryonic lethality was caused by p53 activation, we crossed SIRT1 mutant mice with p53 null mice (Donehower et al., 1992). Our data detected no rescue of embryonic lethality, suggesting that activation of p53 in SIRT1 mutant mice is not a majo r reason for the embryonic lethality.

Moreover, our analysis of public data sets revealed that SIRT1 expression levels are lower than in their normal controls in five types of tumors, including glioblastoma, bladder carcinoma, male germ cell tumors, prostate carcinoma, and ovarian cancers. Our own analysis of 44 breast cancers and 263 HCCs also revealed markedly reduced expression of SIRT1 in these tumors. These data suggest that *SIRT1* may not serve as an oncogene; instead, it may act as a tumor suppressor in these tissues. Consistent with this notion, we demonstrated that $Sirt1^{+/-}$;$p53^{+/-}$ mice develop cancers in multiple tissues. Southern blot and western blot analyses indicated that most tumors still maintained one wild-type allele of *Sirt1*, suggesting that a proper dose of SIRT1 is critical for inhibiting tumorigenesis. We further showed that activation of SIRT1 by resveratrol can partially inhibit tumor formation. It has been demonstrated that resveratrol has chemopreventive activity against various cancers including leukemia, DMBA-induced mammary tumors in rats, skin cancer, and prostate cancer (reviewed in Aggarwal et al., 2004; Delmas et al., 2006). We have also found that resveratrol treatment activates SIRT1 and significantly inhibits growth of BRCA1-associated cancers (R.-H.W. and C.-X.D., unpublished data).

In summary, our analysis of SIRT1 mutant mice has yielded insights regarding the functions of SIRT1. SIRT1 plays an important role in maintenance of heterochromatin structure through deacetylation of histones in vivo. SIRT1 also has an important role in modulating γH2AX, BRCA1, Rad51, and NBS1 foci formation, which are involved in DNA damage repair and the cell-cycle checkpoint. Finally, our observations that impaired SIRT1 function results in tumor formation on a p53 null background and that activation of SIRT1 by resveratrol reduces tumorigenesis provide compelling evidence that *SIRT1* serves as a tumor suppressor gene in mice and some human cancers.

EXPERIMENTAL PROCEDURES

Mating and Genotyping of Mice

Chimeric mice, obtained by injecting targeted $Sirt1^{+/-}$ ES cells into blastocysts, were mated with NIH Black Swiss or C57BL6 females to screen for germline transmission. Male mice bearing germline transmission were mated with female FVB EII-Cre mice (Lakso et al., 1996) to generate complete deletion of *Sirt1* exons 5 and 6. The animals were genotyped by either Southern blot or PCR using primer 1, 5′-TCCTTGCCACAGTCACTCAC-3′; primer 2, 5′-ACAG TCCCATTCCCATACC-3′; and primer 3, 5′-CATCTAAACTTTGTTGGCTGC-3′. Primers 1 and 3 are located within intron 4 and amplify the wild-type allele

(660 bp). Primer 2 is located within exon 7; the combination of primers 1 and 2 amplifies the deleted allele (716 bp). All experiments were approved by the Institutional Animal Care and Use Committee of the National Institute of Diabetes and Digestive and Kidney Diseases.

Proliferation Assays on Embryos

Sirt1$^{+/-}$ mice were mated to generate wild-type (+/+) and mutant (−/−) embryos. At E10.5, E11.5, and E12.5, females were injected with BrdU. Females were euthanized 2 hr postinjection, and embryos were collected, fixed with formalin, and genotyped. Five micrometer sections from paraffin-embedded samples were processed either with BrdU staining (BrdU labeling kit, Zymed) or staining with antibody against phosphorylated histone H3 at Ser10 (pi-H3, Upstate). BrdU- and pi-H3-positive signals were counted from 20 different areas and analyzed by Student's t test.

Chromosome Spreads from Embryos, Primary Tumors, and MEFs

Chromosome spreads from embryos were performed as described previously (Deng and Xu, 2004; Shen et al., 1998). Briefly, embryos were incubated with 100 ng/ml colcemid for 2 hr. The hypotonic treatment was carried out for 20 min at room temperature in 0.56% KCl. The embryos were transferred to methanol:acetic acid (3:1) for fixation. The embryos were then disaggregated under a dissection microscope in 60% acetic acid. The disaggregated embryos were spun down, suspended in methanol:acetic acid, and dropped onto slides. All chromosome spreads were stained with Giemsa, and chromosome number and morphology were assessed under a Leica microscope with a 100× objective and Olympus camera with MagnaFire software (Optronics, purchased from Olympus).

Immunofluorescence Staining

Methanol-fixed MEFs were stained with antibodies against BRCA1 (Turner et al., 2004); Rad51 (Ab-1, Calbiochem); NBS1 (C-19, Santa Cruz); α-tubulin (Sigma); and γH2AX, (me)3-K9 of histone H3, and HP1α (Upstate) using methods described previously (Wang et al., 2004). Images were acquired using either a 63× or 100× lens on an Olympus X81 microscope and processed with Slidebox software. Deparaffinized brain sections from embryos were cooked with Retriever (Cat. 62700-10, Electronic Microscopy Science) in buffer A (citrate buffer, pH 5.0) followed by staining with antibodies against H3 Ac-K9 and/or H4 Ac-K16 (Upstate).

Western Blotting

Western blot was carried out by Li-Cor (Lincoln, NE, USA) with antibodies against BRCA1 (Turner et al., 2004), Rad51 (Ab-1, Calbiochem), NBS1 (C-19, Santa Cruz), H2AX (Cat. 07-627, Upstate), γH2AX (Cat. 05-636, Upstate), CHK2 (Cat. 611571, Becton Dickinson), p53(Ser20) (Cat. 9287, Cell Signaling), p53 (DO-1, Becton Dickinson), SIRT1 (Cat. 07-131, Upstate), Bcl-2 (Sc-783, Santa Cruz), survivin (NB500-201, Novus), histone H3 (Cat. 06-755, Upstate), H3 Ac-K9 (Cat. 07-352, Upstate), histone H4 (Cat. 07-108, Upstate), H4 Ac-K16 (Cat. 06-762, Upstate), β-actin (A5441, Sigma), and α-tubulin (T6074, Sigma).

FACS Analysis of γ-Irradiated MEFs

MEFs at passage 1 were irradiated with different dosages and labeled with BrdU for 24 hr. The cells were fixed with 70% ethanol, stained with anti-BrdU antibodies (Becton Dickinson), and then counterstained with 25 μg/ml propidium iodide. The stained cells were analyzed with a FACSCalibur (Becton Dickinson). The percentage of BrdU-positive cells in the control group was set as 100%.

Comet Assay

Primary MEFs at passage 1 were irradiated with 5 Gy and incubated for 2 hr. Cells were then collected and processed per the manufacturer's protocol (CometAssay 4250-050-K, Trevigen).

RT-PCR

Total RNA was isolated from cells or tissues with STAT-60 following the manufacturer's protocol (Tel-Test, Inc.). cDNA was synthesized with Cells-to-cDNA II (Ambion, Inc.). Primer sequences were as follows:

Mouse Gapdh: forward 5′-ACAGCCGCATCTTCTTGTGC-3′, reverse 5′-CACTTTGCCACTGCAAATGG-3′; mouse SIRT1: forward 5′-TTGTGAAGCTGTTCGTGGAG-3′, reverse 5′-GGCGTGGAGGTTTTTCAGTA-3′; mouse survivin: forward 5′-GTTTGAGTCGTCTTGGCGGAG-3′, reverse 5′-GTCTCCTTCTCTAAGATCCTG-3′; mouse Bcl-2: forward 5′-ATACCTGGGCCACAAGTGAG-3′, reverse 5′-TCTTGTAGGCACCTGCTCCT-3′; mouse p53: forward 5′-CACGTACTCTCCTCCCCTCA-3′; reverse 5′-CTTCTGTACGGCGGTCTCTC-3′.

Resveratrol Treatment

Resveratrol (Cat. 60512A, AKSci) treatment was carried out on 36 female *Sirt1*$^{+/-}$;*p53*$^{+/-}$ mice. Starting at 2 months of age, one group of mice (n = 10) was treated with resveratrol (7.5 μg/ml)-supplemented drinking water daily; another group (n = 10) was treated with carrier (DMSO, 0.015%)-supplemented drinking water daily. The drinking water was kept away from light and changed every 3 days. Resveratrol treatment was maintained for 9 months. The remaining 16 mice were untreated.

Spectral Karyotyping Analysis

SKY analysis was performed as described previously (Padilla-Nash et al., 2006). FISH was performed on metaphase spreads from tumors 785S and 841A by hybridization with whole-chromosome paints against selected target chromosomes that appeared clonally in two or more instances out of ten spreads from SKY analyses.

Clinical Specimens

Tumor and matched normal sample lysates were purchased from Protein Biotechnologies (http://www.proteinbiotechnologies.com/). Twenty microgram aliquots of protein lysates were loaded on gels for western blot analysis. Western blotting was performed with both SIRT1 and tubulin antibodies. The tissue array of breast cancer samples was purchased from US Biomax (Cat. BR1002). Immunohistochemical staining against SIRT1 (Cat. 07-131, Upstate) was carried out with a HistoMouse-SP (AEC) kit (Cat. 95-9544, Zymed). cDNA microarray analysis for 263 HCCs was described previously (Yamashita et al., 2008). Validation of microarray data was carried out by qRT-PCR using the following primers:

SIRT1 forward 5′-GCAGATTAGTAGGCGGCTTG-3′, reverse 5′-TCATCCTCCATGGGTTCTTC-3′; 18S forward 5′-CGGCTACCACATCCAAGGAA-3′, reverse 5′-GCTGGAATTACCGCGGCT-3′.

Use of human tissues was approved by the NIH Office of Human Subjects Research.

SUPPLEMENTAL DATA

The Supplemental Data include Supplemental Experimental Procedures, Supplemental References, two tables, and seven figures and can be found with this article online at http://www.cancercell.org/cgi/content/full/14/4/312/DC1/.

ACKNOWLEDGMENTS

We thank members of the Deng laboratory for critical discussions of this work. We gratefully acknowledge H.M. Padilla-Nash and N. McNeil for assistance with SKY analyses. This research was supported by the Intramural Research Program of the NIH National Institute of Diabetes and Digestive and Kidney Diseases.

Received: February 13, 2008
Revised: June 13, 2008
Accepted: September 4, 2008
Published: October 6, 2008

REFERENCES

Aggarwal, B.B., Bhardwaj, A., Aggarwal, R.S., Seeram, N.P., Shishodia, S., and Takada, Y. (2004). Role of resveratrol in prevention and therapy of cancer: preclinical and clinical studies. Anticancer Res. *24*, 2783–2840.

Antoccia, A., Ricordy, R., Maraschio, P., Prudente, S., and Tanzarella, C. (1997). Chromosomal sensitivity to clastogenic agents and cell cycle

perturbations in Nijmegen breakage syndrome lymphoblastoid cell lines. Int. J. Radiat. Biol. *71*, 41–49.

Aziz, M.H., Afaq, F., and Ahmad, N. (2005). Prevention of ultraviolet-B radiation damage by resveratrol in mouse skin is mediated via modulation in survivin. Photochem. Photobiol. *81*, 25–31.

Baur, J.A., Pearson, K.J., Price, N.L., Jamieson, H.A., Lerin, C., Kalra, A., Prabhu, V.V., Allard, J.S., Lopez-Lluch, G., Lewis, K., et al. (2006). Resveratrol improves health and survival of mice on a high-calorie diet. Nature *444*, 337–342.

Blander, G., and Guarente, L. (2004). The Sir2 family of protein deacetylases. Annu. Rev. Biochem. *73*, 417–435.

Bradbury, C.A., Khanim, F.L., Hayden, R., Bunce, C.M., White, D.A., Drayson, M.T., Craddock, C., and Turner, B.M. (2005). Histone deacetylases in acute myeloid leukaemia show a distinctive pattern of expression that changes selectively in response to deacetylase inhibitors. Leukemia *19*, 1751–1759.

Celeste, A., Difilippantonio, S., Difilippantonio, M.J., Fernandez-Capetillo, O., Pilch, D.R., Sedelnikova, O.A., Eckhaus, M., Ried, T., Bonner, W.M., and Nussenzweig, A. (2003). H2AX haploinsufficiency modifies genomic stability and tumor susceptibility. Cell *114*, 371–383.

Chen, W.Y., Wang, D.H., Yen, R.C., Luo, J., Gu, W., and Baylin, S.B. (2005). Tumor suppressor HIC1 directly regulates SIRT1 to modulate p53-dependent DNA-damage responses. Cell *123*, 437–448.

Cheng, H.L., Mostoslavsky, R., Saito, S., Manis, J.P., Gu, Y., Patel, P., Bronson, R., Appella, E., Alt, F.W., and Chua, K.F. (2003). Developmental defects and p53 hyperacetylation in Sir2 homolog (SIRT1)-deficient mice. Proc. Natl. Acad. Sci. USA *100*, 10794–10799.

Delmas, D., Lancon, A., Colin, D., Jannin, B., and Latruffe, N. (2006). Resveratrol as a chemopreventive agent: a promising molecule for fighting cancer. Curr. Drug Targets *7*, 423–442.

Deng, C., Wynshaw-Boris, A., Zhou, F., Kuo, A., and Leder, P. (1996). Fibroblast growth factor receptor 3 is a negative regulator of bone growth. Cell *84*, 911–921.

Deng, C.X. (2001). Tumorigenesis as a consequence of genetic instability in Brca1 mutant mice. Mutat. Res. *477*, 183–189.

Deng, C.X. (2006). BRCA1: cell cycle checkpoint, genetic instability, DNA damage response, and cancer evolution. Nucleic Acids Res. *34*, 1416–1426.

Deng, C.X., and Xu, X. (2004). Generation and analysis of Brca1 conditional knockout mice. Methods Mol. Biol. *280*, 185–200.

Denu, J.M. (2003). Linking chromatin function with metabolic networks: Sir2 family of NAD(+)-dependent deacetylases. Trends Biochem. Sci. *28*, 41–48.

Donehower, L.A., Harvey, M., Slagle, B.L., McArthur, M.J., Montgomery, C.A., Jr., Butel, J.S., and Bradley, A. (1992). Mice deficient for p53 are developmentally normal but susceptible to spontaneous tumours. Nature *356*, 215–221.

Ferguson, D.O., and Alt, F.W. (2001). DNA double strand break repair and chromosomal translocation: lessons from animal models. Oncogene *20*, 5572–5579.

Firestein, R., Blander, G., Michan, S., Oberdoerffer, P., Ogino, S., Campbell, J., Bhimavarapu, A., Luikenhuis, S., de Cabo, R., Fuchs, C., et al. (2008). The SIRT1 deacetylase suppresses intestinal tumorigenesis and colon cancer growth. PLoS ONE *3*, e2020.

Gasser, S.M., and Cockell, M.M. (2001). The molecular biology of the SIR proteins. Gene *279*, 1–16.

Guarente, L. (2000). Sir2 links chromatin silencing, metabolism, and aging. Genes Dev. *14*, 1021–1026.

Haigis, M.C., and Guarente, L.P. (2006). Mammalian sirtuins–emerging roles in physiology, aging, and calorie restriction. Genes Dev. *20*, 2913–2921.

Harper, C.E., Patel, B.B., Wang, J., Arabshahi, A., Eltoum, I.A., and Lamartiniere, C.A. (2007). Resveratrol suppresses prostate cancer progression in transgenic mice. Carcinogenesis *28*, 1946–1953.

Hida, Y., Kubo, Y., Murao, K., and Arase, S. (2007). Strong expression of a longevity-related protein, SIRT1, in Bowen's disease. Arch. Dermatol. Res. *299*, 103–106.

Howitz, K.T., Bitterman, K.J., Cohen, H.Y., Lamming, D.W., Lavu, S., Wood, J.G., Zipkin, R.E., Chung, P., Kisielewski, A., Zhang, L.L., et al. (2003). Small molecule activators of sirtuins extend Saccharomyces cerevisiae lifespan. Nature *425*, 191–196.

Huffman, D.M., Grizzle, W.E., Bamman, M.M., Kim, J.S., Eltoum, I.A., Elgavish, A., and Nagy, T.R. (2007). SIRT1 is significantly elevated in mouse and human prostate cancer. Cancer Res. *67*, 6612–6618.

Jeong, J., Juhn, K., Lee, H., Kim, S.H., Min, B.H., Lee, K.M., Cho, M.H., Park, G.H., and Lee, K.H. (2007). SIRT1 promotes DNA repair activity and deacetylation of Ku70. Exp. Mol. Med. *39*, 8–13.

Kim, J.E., Chen, J., and Lou, Z. (2008). DBC1 is a negative regulator of SIRT1. Nature *451*, 583–586.

Kobayashi, J. (2004). Molecular mechanism of the recruitment of NBS1/hMRE11/hRAD50 complex to DNA double-strand breaks: NBS1 binds to gamma-H2AX through FHA/BRCT domain. J. Radiat. Res. (Tokyo) *45*, 473–478.

Lagouge, M., Argmann, C., Gerhart-Hines, Z., Meziane, H., Lerin, C., Daussin, F., Messadeq, N., Milne, J., Lambert, P., Elliott, P., et al. (2006). Resveratrol improves mitochondrial function and protects against metabolic disease by activating SIRT1 and PGC-1alpha. Cell *127*, 1109–1122.

Lain, S., Hollick, J.J., Campbell, J., Staples, O.D., Higgins, M., Aoubala, M., McCarthy, A., Appleyard, V., Murray, K.E., Baker, L., et al. (2008). Discovery, in vivo activity, and mechanism of action of a small-molecule p53 activator. Cancer Cell *13*, 454–463.

Lakso, M., Pichel, J.G., Gorman, J.R., Sauer, B., Okamoto, Y., Lee, E., Alt, F.W., and Westphal, H. (1996). Efficient in vivo manipulation of mouse genomic sequences at the zygote stage. Proc. Natl. Acad. Sci. USA *93*, 5860–5865.

Li, T., Fan, G.X., Wang, W., and Yuan, Y.K. (2007). Resveratrol induces apoptosis, influences IL-6 and exerts immunomodulatory effect on mouse lymphocytic leukemia both in vitro and in vivo. Int. Immunopharmacol. *7*, 1221–1231.

Lim, C.S. (2006). SIRT1: tumor promoter or tumor suppressor? Med. Hypotheses *67*, 341–344.

McAinsh, A.D., Scott-Drew, S., Murray, J.A., and Jackson, S.P. (1999). DNA damage triggers disruption of telomeric silencing and Mec1p-dependent relocation of Sir3p. Curr. Biol. *9*, 963–966.

McBurney, M.W., Yang, X., Jardine, K., Hixon, M., Boekelheide, K., Webb, J.R., Lansdorp, P.M., and Lemieux, M. (2003). The mammalian SIR2alpha protein has a role in embryogenesis and gametogenesis. Mol. Cell. Biol. *23*, 38–54.

Mills, K.D., Sinclair, D.A., and Guarente, L. (1999). MEC1-dependent redistribution of the Sir3 silencing protein from telomeres to DNA double-strand breaks. Cell *97*, 609–620.

Nagy, A., Rossant, J., Nagy, R., Abramow-Newerly, W., and Roder, J.C. (1993). Derivation of completely cell culture-derived mice from early-passage embryonic stem cells. Proc. Natl. Acad. Sci. USA *90*, 8424–8428.

Padilla-Nash, H.M., Barenboim-Stapleton, L., Difilippantonio, M.J., and Ried, T. (2006). Spectral karyotyping analysis of human and mouse chromosomes. Nat. Protoc. *1*, 3129–3142.

Paull, T.T., Rogakou, E.P., Yamazaki, V., Kirchgessner, C.U., Gellert, M., and Bonner, W.M. (2000). A critical role for histone H2AX in recruitment of repair factors to nuclear foci after DNA damage. Curr. Biol. *10*, 886–895.

Rodgers, J.T., Lerin, C., Haas, W., Gygi, S.P., Spiegelman, B.M., and Puigserver, P. (2005). Nutrient control of glucose homeostasis through a complex of PGC-1alpha and SIRT1. Nature *434*, 113–118.

Saunders, L.R., and Verdin, E. (2007). Sirtuins: critical regulators at the crossroads between cancer and aging. Oncogene *26*, 5489–5504.

Shen, S.X., Weaver, Z., Xu, X., Li, C., Weinstein, M., Chen, L., Guan, X.Y., Ried, T., and Deng, C.X. (1998). A targeted disruption of the murine Brca1 gene causes gamma-irradiation hypersensitivity and genetic instability. Oncogene *17*, 3115–3124.

Stunkel, W., Peh, B.K., Tan, Y.C., Nayagam, V.M., Wang, X., Salto-Tellez, M., Ni, B., Entzeroth, M., and Wood, J. (2007). Function of the SIRT1 protein deacetylase in cancer. Biotechnol. J. *2*, 1360–1368.

Tsukamoto, Y., Kato, J., and Ikeda, H. (1997). Silencing factors participate in DNA repair and recombination in Saccharomyces cerevisiae. Nature *388*, 900–903.

Turner, J.M., Aprelikova, O., Xu, X., Wang, R., Kim, S., Chandramouli, G.V., Barrett, J.C., Burgoyne, P.S., and Deng, C.X. (2004). BRCA1, histone H2AX phosphorylation, and male meiotic sex chromosome inactivation. Curr. Biol. *14*, 2135–2142.

Vaquero, A., Sternglanz, R., and Reinberg, D. (2007). NAD+-dependent deacetylation of H4 lysine 16 by class III HDACs. Oncogene *26*, 5505–5520.

Wang, R.H., Yu, H., and Deng, C.X. (2004). A requirement for breast-cancer-associated gene 1 (BRCA1) in the spindle checkpoint. Proc. Natl. Acad. Sci. USA *101*, 17108–17113.

Whitsett, T., Carpenter, M., and Lamartiniere, C.A. (2006). Resveratrol, but not EGCG, in the diet suppresses DMBA-induced mammary cancer in rats. J. Carcinog. *5*, 15.

Xu, X., Qiao, W., Linke, S.P., Cao, L., Li, W.M., Furth, P.A., Harris, C.C., and Deng, C.X. (2001). Genetic interactions between tumor suppressors Brca1 and p53 in apoptosis, cell cycle and tumorigenesis. Nat. Genet. *28*, 266–271.

Yamashita, T., Forgues, M., Wang, W., Kim, J.W., Ye, Q., Jia, H., Budhu, A., Zanetti, K.A., Chen, Y., Qin, L.X., et al. (2008). EpCAM and alpha-fetoprotein expression defines novel prognostic subtypes of hepatocellular carcinoma. Cancer Res. *68*, 1451–1461.

Yuan, Z., Zhang, X., Sengupta, N., Lane, W.S., and Seto, E. (2007). SIRT1 regulates the function of the Nijmegen breakage syndrome protein. Mol. Cell *27*, 149–162.

Zhao, W., Kruse, J.P., Tang, Y., Jung, S.Y., Qin, J., and Gu, W. (2008). Negative regulation of the deacetylase SIRT1 by DBC1. Nature *451*, 587–590.